



Exploring visible spectrum wavelengths in light transmission through wood material

Juliette Boivin¹ · Damien Teyssieux² · Luc Froehly² · Stéphane Girardon¹ · Louis Denaud¹

Received: 23 April 2024 / Accepted: 22 July 2024 / Published online: 17 August 2024
© The Author(s) 2024

Abstract

Wood is a multiscale heterogeneous natural composite material with properties depending on its growing conditions and its genetic heritage. This variability is challenging for industries that work to perform homogeneous and reliable products. In industry, different non-destructive testing methods are in use to classify, grade, and select wood products to optimize their usage. Among them, the use of lasers to detect fiber orientation with different wavelengths. This orientation significantly influences the mechanical behavior of wood, including stress limits and stiffness. According to our knowledge, the use of laser diffusion still is limited to grain angle measurement. Our objective in this paper is to realize transmission light scattering maps for wood samples from several wood species (poplar, oak, Douglas fir, beech), and then identify the most suitable wavelength to study light diffusion in wood, depending on the property that will be measured. A supercontinuum laser is used over a wavelength range from 500 to 800 nm, allowing precise adjustment of the wavelengths. It was found that near-infrared light better scatters in the studied wood species than lower wavelength. However, the wavelength that gives the best contrast between earlywood and latewood depends on the sample studied and is not necessarily in the near infrared rays.

✉ Juliette Boivin
juliette.boivin@ensam.eu

Damien Teyssieux
damien.teyssieux@femto-st.fr

Luc Froehly
luc.froehly@univ-fcomte.fr

Stéphane Girardon
stephane.girardon@ensam.eu

Louis Denaud
louis.denaud@ensam.eu

¹ Arts et Metiers Institute of Technology, LABOMAP, Université Bourgogne Franche-Comté, F-71250 Cluny, France

² Institut FEMTO-ST, CNRS UMR 6174, Université de Franche-Comté, Besançon, France

Introduction

Wood is a living material, influenced by its growth conditions, which makes it a highly variable material. It has a complex multi-scale structure (Schoch et al. 2004; Trouy 2015), and its anatomical structure depends on the species to which it belongs. Softwoods are made up of cells called tracheids. They are 3–5 mm long and 15–80 μm wide, depending on their position in the growth ring. Hardwoods, on the other hand, are made up of more differentiated cells, the vessels, which are very large in diameter and serve to conduct sap, while the fibres contribute to mechanical strength. The fibres are between 1 and 2 mm long and between 10 and 50 μm wide (Tsoumis 1991; Niemz et al. 2023). This complexity poses challenges in industrializing the material to achieve standardized properties. In particular, woods that grew up in temperate regions are more likely to have large knots or strong density gradients, so the use of non-destructive testing is all the more important to enhance the value of this secondary quality resource. These characteristics should be measured using efficient and fast non-destructive methods. Among the different physical properties that can be measured, the local density and the moisture content are very important since they influence the mechanical wood properties. To measure the wood density with accuracy at an industrial scale, X-ray appears to be the most used technology (Benson-Cooper and Knowles 1982; Funt 1985; Viguiier 2015). Terahertz wave measurement technology also offers interesting prospects for measuring moisture and density in wood (Inagaki et al. 2014).

Apart from its local density, one of the most important parameters of wood heterogeneity is the orientation of its fibers, as a variation of this orientation has a significant influence on its local mechanical properties (Hankinson 1921). Understanding the local orientation of wood grain is essential for a comprehensive assessment of the wood's local strength characteristics, as discussed in previous studies. This knowledge is essential for predicting bending strength and stiffness, a point underscored by Olsson et al. (2013). Additionally, it serves as valuable insight into the identification of specific wood defects, including knots, which was studied by Tormanen and Makynen (2009), and the determination of the pith's location, as explored by Briggert et al. (2016).

The fiber direction at the surface of wood can be determined using the so-called tracheid effect (Nyström 2003; Kienle et al. 2008): when a laser beam illuminates a wooden surface, the light is scattered and leads to a halo of light with an elliptical shape whose major axis follows the wood fibers (Fig. 1). The light ellipse visible at the surface of the sample is then captured by a camera and the image processed.

The majority of studies investigating the “tracheid effect” has predominantly concentrated on a single wood species or a limited number of species. These studies consistently utilize a laser with a fixed wavelength, typically ranging between 630 and 680 nm, and operate on the wood's surface (Nyström 2003; Hu et al. 2004; Simonaho et al. 2004; Jolma and Mäkynen 2008; Tormanen and Makynen 2009; Briggert et al. 2018). Several studies have demonstrated that the elliptical

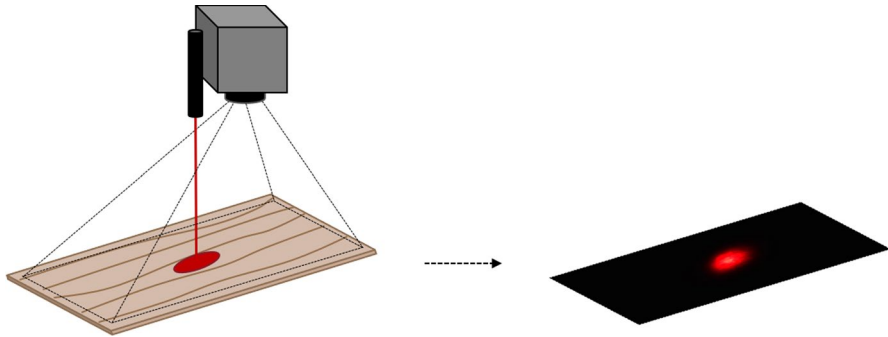


Fig. 1 Illustration of tracheid effect

appearance and the information extractable from it may vary depending on the wood species and its physical specific characteristics [Example of the difference in the appearance of the light ellipse on earlywood (Fig. 2a) and latewood (Fig. 2b)]. In other words, the elliptical shape appears to be strongly correlated with wood physical properties but the underlying mechanism is never explained.

Besseau et al. (2020) showed that the appearance of the ellipses obtained varied according to the species used and the moisture conditions of the sample. Purba et al. (2020) showed that the area of the ellipse increased as its moisture content increased. Tan et al. (2023) compared the ellipses obtained with two lasers of different wavelengths and assessed the relevance of their use, taking into account the cost and material constraints associated with industrial use. All these studies demonstrate the direct link that exists between the wood microstructure and wood composition at the cellular scale and the phenomenon of light wave diffusion. A better understanding and explanation of the light diffusion mechanism could thus allow

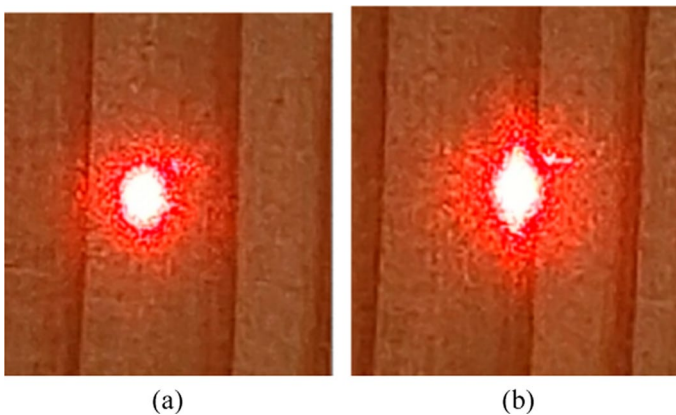


Fig. 2 Illustration on a Douglas fir (*Pseudotsuga menziesii*) sample of the difference in appearance of the scattering ellipse depending on where the laser is aimed (a) on earlywood (b) on latewood in the LR plane

for the measurement of further properties beyond fiber orientation, such as moisture content or density. Indeed, the literature is sparse in the field of light transmission through wood (Sugimoto et al. 2018). This mechanism is necessary to understand the proportions of light that are reflected, absorbed, scattered, and transmitted. This is in order to optimize the usable light intensity once the light has passed through the wood material while ensuring sufficient interaction with it. It would be interesting to better understand and explain the mechanisms governing this “tracheid effect” in order to fully exploit it, not only for determining the direction of fibers projected onto the observed surface since its reflection.

As a result, this study aims to examine how the wavelength affects light transmittance. The goal is to identify a specific wavelength that can emphasize particular wood properties using the tracheid effect, while staying within visible wavelengths to prioritize both operator safety and cost-effectiveness.

In the following section, the wood samples used and the different elements of the set-up used to make the measurements are presented. The results obtained show better transmittance in the near-infrared range for the four studied species, and a noticeable contrast between earlywood and latewood around 600 nm. Their representativeness and reliability will be discussed.

Materials and methods

Wood samples

The studied species are beech (*Fagus sylvatica*), Douglas fir (*Pseudotsuga menziesii*), poplar (*Populus*), and oak (*Quercus*). These species are chosen due to their encompassment of diverse microstructures, including softwood, diffuse pore and initial porous zone hardwood species. Additionally, these four species constitute the vast majority of locally available wood types in Burgundy (France). Two different grain orientations, radial and tangential, are studied among the three principal planes of wood (Fig. 3), to analyze the most common situation available in the wood industry (approximatively radial and tangential in sawing, tangential in peeling).

For each of the two orientations and four species, sawn timber was planed until samples with a thickness of 1 mm and 3 mm were obtained. They were then sawn to a width and height of 50 x 50 mm. A total of 16 samples were produced.

Experimental set-up

The purpose of this setup is to capture the light transmitted through the sample by placing it on a movable support. The operation is repeated at various positions of the specimen to observe the influence of wood structure on diffusion.

Figure 4a shows a schematic of the experimental setup. The light source is a supercontinuum laser (Leukos electro-VIS), emitting within the spectral wavelength range of 400–2400 nm. The laser operates in a single-transverse mode, with a total power of 1 W. The power is manually adjustable. The pump source for

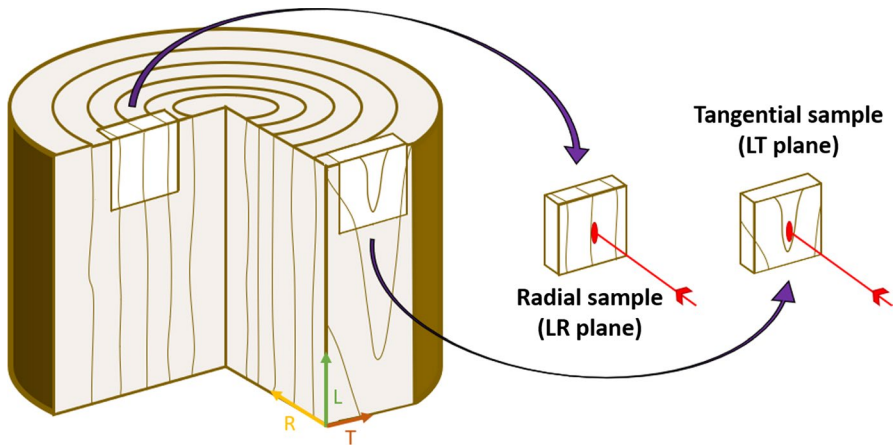
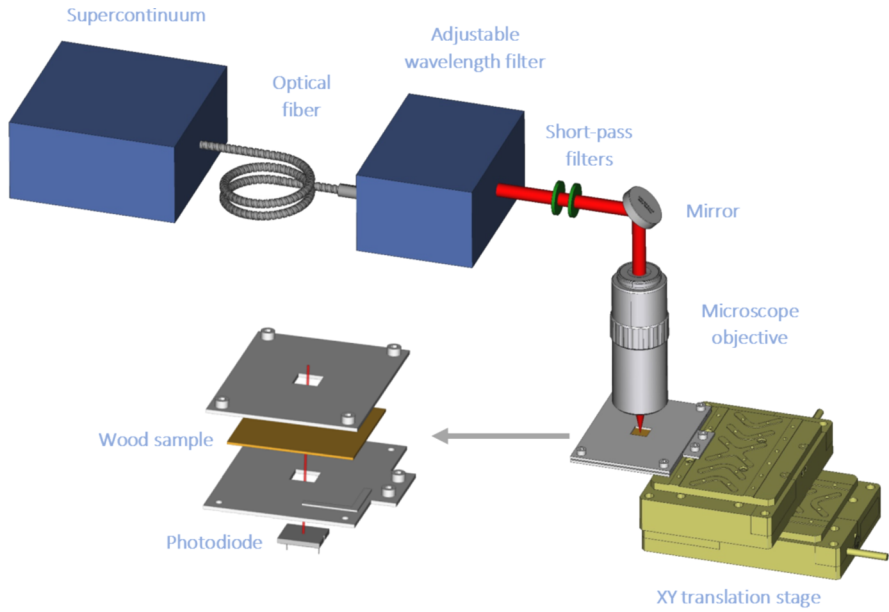


Fig. 3 Representation of the orientation of the samples used and the orientation of the laser beam incident on them

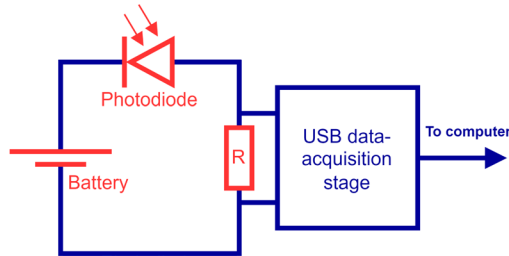
the supercontinuum is a high-power pulsed laser diode operating at 1064 nm. The focused beam has a diameter of approximately 10 micrometers when it reaches the sample. The source is followed by an adjustable wavelength filter (Leukos Bebop) controlled by a computer. In all experiments, the bandwidth is set to 10 nm, with the central wavelength varying from 500 to 800 nm in 25 nm increments. To mitigate the high power from the pump source, two additional short-pass filters (Thorlabs NENIR20A) are positioned behind the adjustable filter.

The sample is clamped between two thin aluminum plates, each with a square central opening measuring 10 mm by 10 mm. A long working distance objective (MPLFLN20x) is employed to focus the light onto the surface of the sample. A large sensitive surface photodiode (Thorlabs FDS10X10) (10 x 10 mm) allows for the measurement of the transmitted light power through the sample. The laser light is directed onto the center of the sensitive surface of the photodiode. The photodiode is positioned as close as possible to the sample. Tests have shown that in this configuration, all the light is collected by the photodiode despite the diffusivity caused by the wood. Two translation stages (PI V-528.1AA) allow scanning the sample perpendicularly to the laser. In this configuration, only the sample moves, while the laser and the photodiode remain fixed. The entire setup is integrated into a fully light-tight box.

The photodiode is made of silicon (350–1100 nm spectral wavelength range) and exhibits a dark current of 200 pA at ambient temperature. It is reverse-biased with a series load resistor (Fig. 4b). In this configuration, the photocurrent is proportional to the incident light power. Thus, the voltage across the resistance is proportional to the incident light power and sent to the computer via a 14 bits National Instrument USB data-acquisition interface. The spectral responsivity $S(\lambda)$ of the photodiode is provided in the datasheet but has been measured for the wavelength range from 500 to 800 nm. The output power is determined



(a) Experimental set-up for measuring the transmittance of wood samples



(b) Process of acquiring transmittance data via the photodiode

Fig. 4 Experimental set-up and acquisition process

by measuring the voltage to the resistor terminals. The value of the resistor is adjusted so that the photodiode is never in a saturation state.

Methods

The transmittance of the sample is defined as the ratio between the output light power and the input light power:

$$T_{r,wood} = \frac{P_{out}}{P_{in}} \tag{1}$$

where P_{out} is the output power measured by the photodiode and P_{in} is the input power measured at the output of the microscope objective (just before the sample).

P_{in} is measured by an optical powermeter (Thorlabs PM100D) not shown on the schematic. P_{out} is defined by:

$$P_{out} = \frac{V}{S(\lambda)R} \quad (2)$$

where V is the measured voltage across the resistor, $S(\lambda)$ is the spectral responsivity of the photodiode and R the value of the resistor. Thus, the sample transmittance is determined by:

$$T_{r,wood} = \frac{V}{P_{in}S(\lambda)R} \quad (3)$$

Before each sample scan, the output power P_{in} from the objective is measured at every wavelength. Subsequently, the wavelength is held constant while the sample undergoes precise movement using point-to-point translation stages. At each spatial coordinate, the voltage value V across the resistance is recorded. Consequently, the output power P_{out} is determined for each coordinate, leading to the calculation of the transmittance. These procedural steps are iterated across the entire spectrum of wavelengths, spanning from 500 to 800 nm with increments of 25 nm. Moreover, for each wood species examined and each wavelength, a surface area measuring 10×10 mm is scanned with a resolution of 0.1 mm. In order to optimize measurement time, 10 consecutive measurements are performed in the range of 500–650 nm (range with low signal) in the way to increase signal to noise ratio. For the range of 650–800 nm, only 2 measurements are taken per point (range with the highest signal).

Results and discussion

During measurements, the assumption was made that light passing through the wood exits at the same location on the other side. However, depending on how light is reflected and absorbed within the wood, this assumption may not hold true (Fig. 5a).

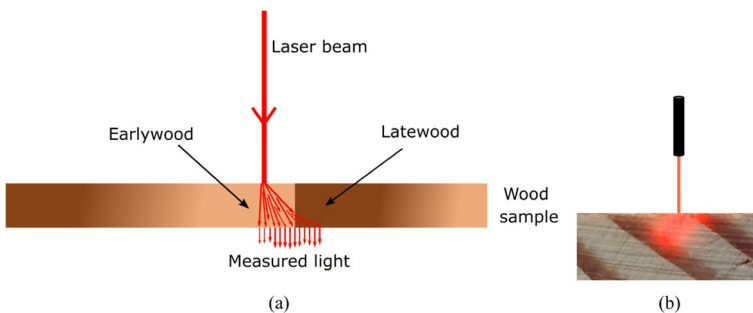
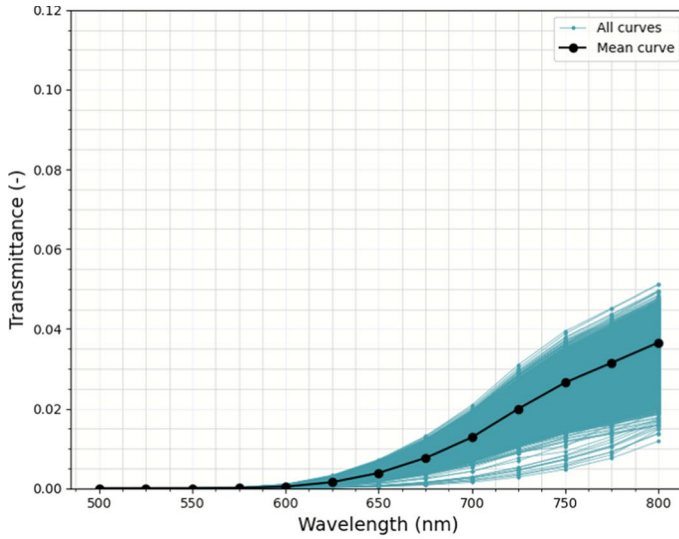
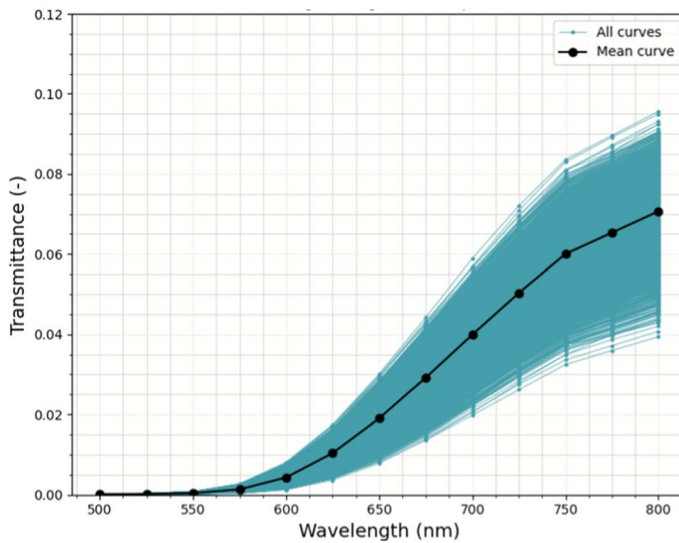


Fig. 5 **a** Impact of light diffusion in wood on the measurement and **b** example of light scattering variation in a Douglas fir sample



(a) Douglas radial sample



(b) Douglas tangential sample

Fig. 6 Transmission ($T_{r,wood}$) evolution at multiple points of radial (a) and tangential (b) Douglas fir samples as a function of wavelength

The curves illustrating the evolution of transmittance as a function of wavelength at each point of the scan for the 1 mm radial Douglas fir sample are visible in Fig. 6a and b. A clear difference is observed between the average curves for the two wood orientations. However, in both cases, the measurements obtained exhibit significant noise, even though the average remains well centered within the cluster of curves.

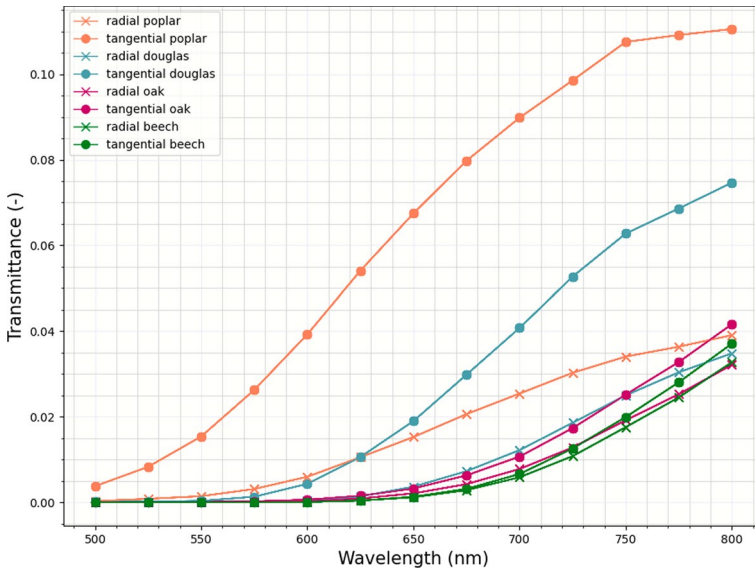


Fig. 7 Transmittance ($T_{r,wood}$) of 1 mm thick samples

The averaged transmittance values of the measurement campaign with respect to the emitted wavelength is shown on Fig. 7. It can be seen that the 8 curves show the same general trend, i.e. a higher transmittance in the near infrared (800 nm) than in the near ultraviolet (500 nm). A slight difference in the shape of the curves is visible between poplar/Douglas fir and oak/beech. The transmittance of the first two species seems to start stabilising or at least growing more slowly around 800 nm while the transmittance of the other two species continues to grow. This may simply be a translation, but measurements beyond 800 nm are needed to confirm this. The transmittance in tangential section is higher than the transmittance in radial section for all the four species. The transmittance ratio for the two orientations is up to 2 at 800 nm for Douglas fir and poplar. This ratio is smaller for oak and beech, with a maximum of approximately 1.2 at 800 nm.

The results obtained seem to show trends, but are not generalizable and require further investigation, given that they average values for earlywood and latewood and may therefore overlook local particularities, so more complementary measurements on smaller, homogeneous areas within the same sample are needed.

The maps obtained allow us to recognize patterns visible to the naked eye (Fig. 8), such as wooden rays or color differences between earlywood and latewood. The hypothesis of greater scattering in the near infrared than in the lower wavelengths is confirmed on the measured transmittance maps (Fig. 9) which is made.

However, better transmission does not necessarily mean better highlighting on the specificities of the sample: Fig. 10 shows two transmittance maps made on the same sample and on the same grid of points with two different wavelengths (600 and 800 nm). While the overall transmittance of the 800 nm map is higher than that of the 600 nm map, the latter highlights contrasts between the rings that are

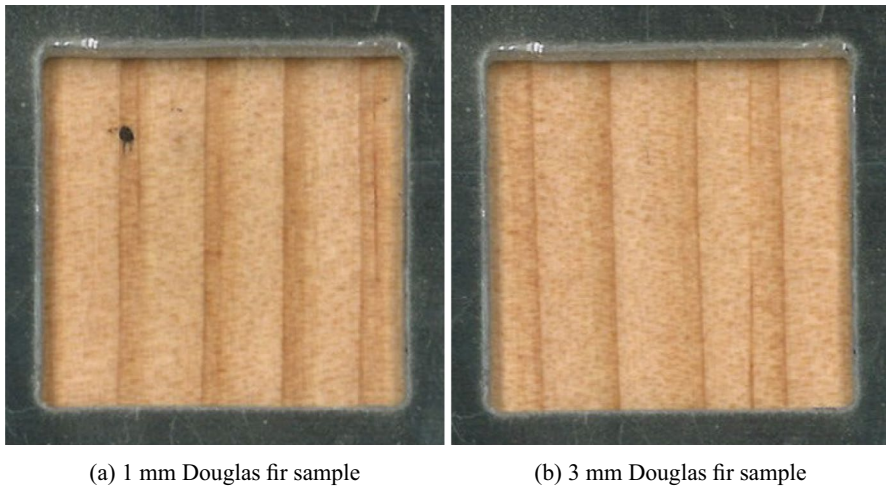


Fig. 8 Representation of the scanned Douglas fir samples within the setup mount

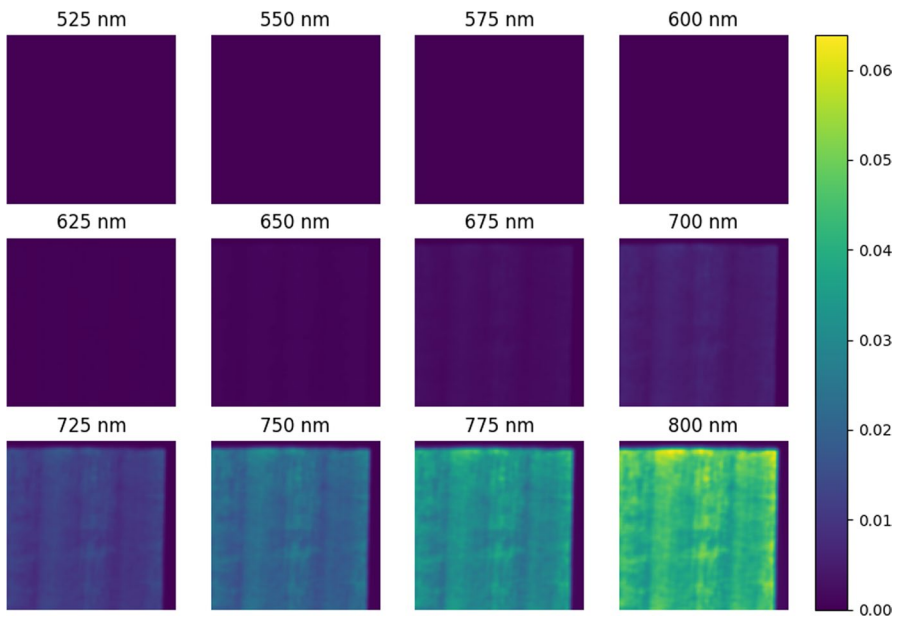


Fig. 9 Transmittance ($T_{r,wood}$) of the 3 mm thick Douglas fir sample at different wavelengths

not visible on the other map. This means that within the context of ring detection or sawn boards position within the log (Li et al. 2023), the use of lighting at this wavelength could improve measurements. Given that wood is a biological material, it can be assumed that interactions are specific around 600–650 nm, as is the case, for example, with the skin (Cheong et al. 1990). A unique interaction

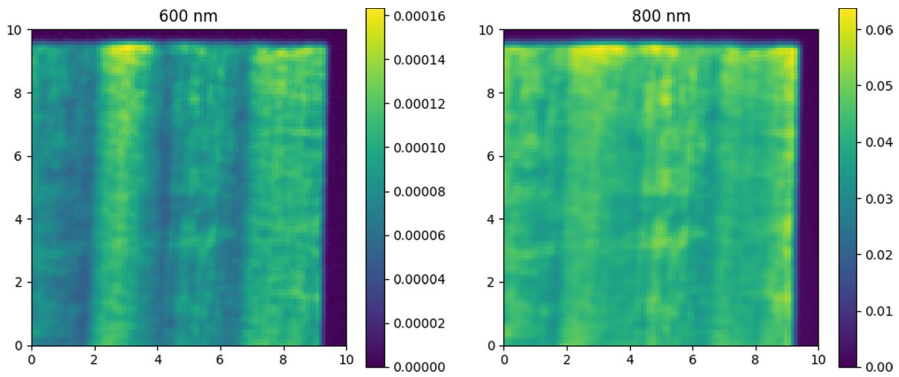
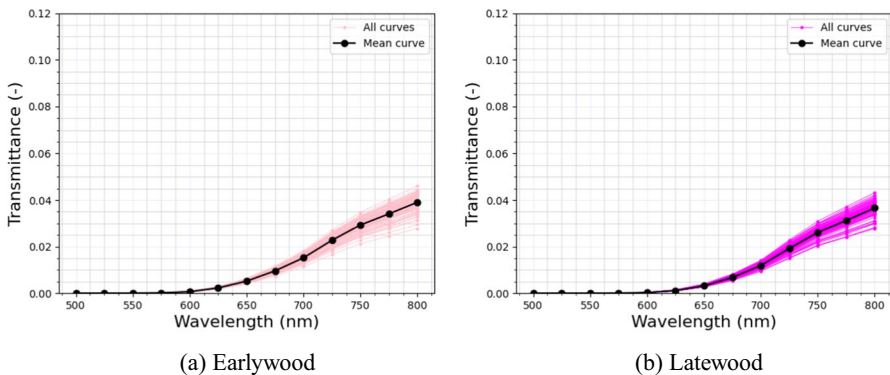


Fig. 10 Transmittance ($T_{r,wood}$) maps at a 600 nm and a 800 nm wavelength for the 3 mm thick Douglas fir in the LR plane

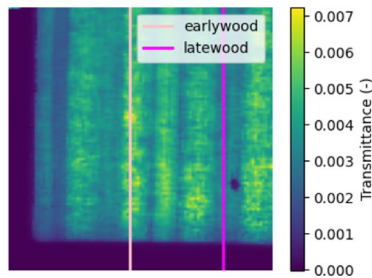
between the refractive indices of wood and air in this range of wavelengths can also be considered.

Specifically, two lines corresponding to earlywood and latewood were isolated from the radial 1 mm Douglas fir sample measurements, and these are formalized in the map shown in Fig. 11c. The bundles of curves corresponding to the evolution



(a) Earlywood

(b) Latewood



(c) Transmittance map

Fig. 11 Transmittance ($T_{r,wood}$) evolution for one line of **a** earlywood, **b** latewood, **c** transmittance map

of transmittance as a function of wavelength are shown for the earlywood line in Fig. 11a and for the latewood line in Fig. 11b.

It is noteworthy that among the four woods studied, Douglas fir exhibits a significant contrast between earlywood and latewood rings, making it the wood most likely to highlight transmittance differences associated with this parameter, if they exist. The average curves obtained for earlywood and latewood appear similar, suggesting no apparent correlation between wood type and transmittance measurements. However, it should be noted that transmittance measurements, conducted using a photodiode, involve averaging the diffusion ellipse without considering its shape and specific characteristics.

We also looked at the evolution of transmittance as a function of wavelength for a measurement line parallel to the wood rings and a line perpendicular to them, shown in Fig. 12c. A dark pencil point at the intersection of the two lines, vertical and horizontal, serves as a control. The curves in Fig. 12a and b, corresponding respectively to the horizontal and vertical lines of the mapping, are again scattered around 800 nm. The few curves that stand out from the beam in both cases correspond to the pencil point values. While we might expect more variability in the cluster of curves on the horizontal line, given that the area covered is made up of woods of widely varying densities, this is not what is observed. The variability of the vertical

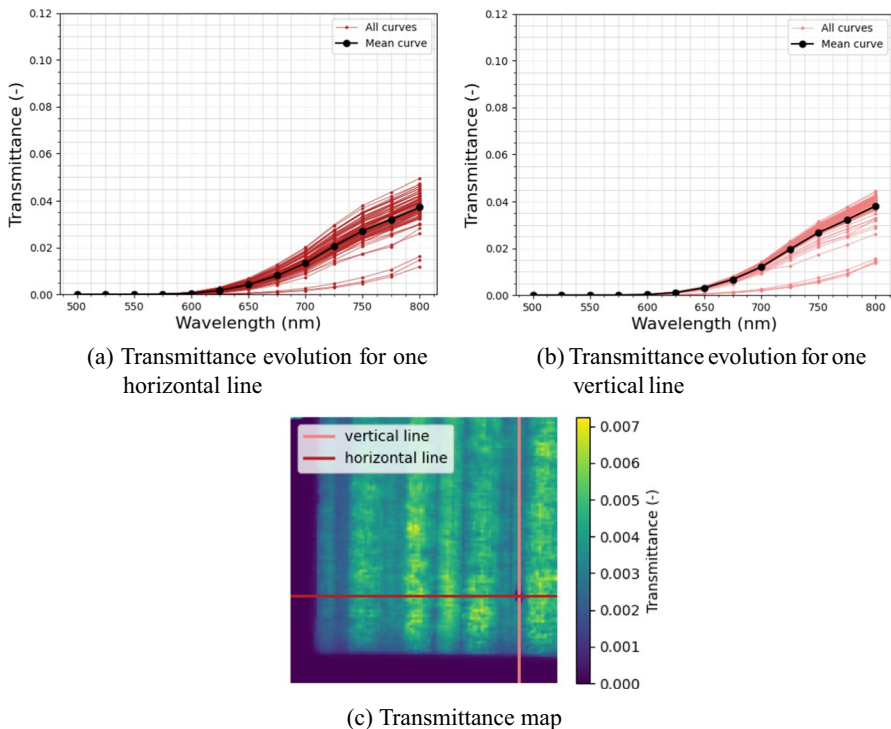


Fig. 12 Transmittance ($T_{r,wood}$) evolution for one line of **a** horizontal, **b** vertical, **c** transmittance map

line is similar to that of the horizontal line, while the area covered is homogeneous in density.

Given that the measurements are carried out using a photodiode, both the local resolution and the provided information are limited. Additional measurements are therefore necessary to reach conclusions. A larger number of samples need to be studied to ensure the reliability of the measured values, especially in discriminating more finely the impact of the transition from earlywood to latewood on transmittance.

Conclusion

In this study, we conducted transmittance measurements on samples of various species with distinct microstructures across a wavelength range from 500 to 800 nm. These measurements revealed an overall improvement in transmittance at 800 nm for the four species under investigation. However, the measurements exhibited significant noise. Notably, a heightened contrast between earlywood and latewood was observed for specific species at 625 nm. The origin of this contrast has not yet been determined, although it is plausible that it arises from refractive indices.

In future research, efforts will focus on comprehending the observed differences by combining experiments with simulations. This involves examining a wider variety of wood species and exploring additional factors like moisture content and density. Additionally, the next experimental phase includes replacing the photodiode with a lens and a camera to analyze scattering ellipses rather than just transmittance values. Simultaneously, light scattering simulations in simplified wood models are planned to explore parameters influencing the tracheid effect and to compare simulation outcomes with experimental data.

Acknowledgements This work is supported by the “Investissement d’avenir” program, ISITE-BFC project (contract ANR-15-IDEX-003), and by a doctoral scholarship and a seeding project funded by the CRBF.

Funding Open access funding provided by Arts et Metiers Institute of Technology.

Open Access This article is licensed under a Creative Commons Attribution 4.0 International License, which permits use, sharing, adaptation, distribution and reproduction in any medium or format, as long as you give appropriate credit to the original author(s) and the source, provide a link to the Creative Commons licence, and indicate if changes were made. The images or other third party material in this article are included in the article’s Creative Commons licence, unless indicated otherwise in a credit line to the material. If material is not included in the article’s Creative Commons licence and your intended use is not permitted by statutory regulation or exceeds the permitted use, you will need to obtain permission directly from the copyright holder. To view a copy of this licence, visit <http://creativecommons.org/licenses/by/4.0/>.

References

- Benson-Cooper D, Knowles R (1982) Computed tomographic scanning for the detection of defects within logs. Forest Research Institute, New York
- Besseau B, Pot G, Collet R, Viguier J (2020) Influence of wood anatomy on fiber orientation measurement obtained by laser scanning on five European species. *J Wood Sci* 66(1):74
- Briggert A, Olsson A, Oscarsson J (2016) Three-dimensional modelling of knots and pith location in Norway spruce boards using tracheid-effect scanning. *Eur J Wood Prod* 74:725–739
- Briggert A, Hu M, Olsson A, Oscarsson J (2018) Tracheid effect scanning and evaluation of in-plane and out-of-plane fiber direction in Norway spruce timber. *Wood Fiber Sci* 50:411–429. <https://doi.org/10.22382/wfs-2018-053>
- Cheong W-F, Prah SA, Welch AJ (1990) A review of the optical properties of biological tissues. *IEEE J Quantum Electron* 26(12):2166–2185
- Funt V (1985) A computer vision system that analyses ct-scans of sawlogs. In: Proceedings of IEEE computer society conference on computer vision and pattern recognition, pp 9–13
- Hankinson R (1921) Investigation of crushing strength of spruce at varying angles of grain. *Air Serv Inf Circ* 3(259):130
- Hu C, Tanaka C, Ohtani T (2004) On-line determination of the grain angle using ellipse analysis of the laser light scattering pattern image. *J Wood Sci* 50:321–326
- Inagaki T, Ahmed B, Hartley I, Tsuchikawa S, Reid M (2014) Simultaneous prediction of density and moisture content of wood by terahertz time domain spectroscopy. *J Infrared Millim Terahertz Waves*. <https://doi.org/10.1007/s10762-014-0095-7>
- Jolma IP, Mäkyänen AJ (2008) The detection of knots in wood materials using the tracheid effect. In: *Advanced laser technologies 2007*, vol 7022. SPIE, pp 143–151
- Kienle A, D'Andrea C, Foschum F, Taroni P, Pifferi A (2008) Light propagation in dry and wet softwood. *Opt Express* 16:9895–906. <https://doi.org/10.1364/OE.16.009895>
- Li X, Pot G, Ngo P, Viguier J, Penvern H (2023) An image processing method to recognize position of sawn boards within the log. *Wood Sci Technol* 57(6):1401–1420
- Niemz P, Teischinger A, Sandberg D (2023) Springer handbook of wood science and technology. Springer, Berlin
- Nyström J (2003) Automatic measurement of fiber orientation in softwoods by using the tracheid effect. *Comput Electron Agric* 41:91–99. [https://doi.org/10.1016/S0168-1699\(03\)00045-0](https://doi.org/10.1016/S0168-1699(03)00045-0)
- Olsson A, Oscarsson J, Serrano E, Källsner B, Johansson M, Enquist B (2013) Prediction of timber bending strength and in-member cross-sectional stiffness variation on basis of local wood fibre orientation. *Eur J Wood Wood Prod* 71(3):319–333
- Purba CYC, Viguier J, Denaud L, Marcon B (2020) Contactless moisture content measurement on green veneer based on laser light scattering patterns. *Wood Sci Technol* 54(4):891–906
- Schoch W, Heller I, Schweingruber FH, Kienast F (2004) Wood anatomy of central European Species. <https://www.woodanatomy.ch>
- Simonaho S-P, Palviainen J, Tolonen Y, Silvennoinen R (2004) Determination of wood grain direction from laser light scattering pattern. *Opt Lasers Eng* 41(1):95–103
- Sugimoto H, Kawabuchi S, Sugimori M, Gril J (2018) Reflection and transmission of visible light by sugi wood: effects of cellular structure and densification. *J Wood Sci* 64:738–744
- Tan CO, Ng SC, Yap HJ, Mustapa MZ, Usop Z, Mâ Fauthan, Mahalil KB, Liew SJ (2023) Feasibility of detecting “tracheid effect” on tropical hardwood (light red meranti, shorea spp.) using 650 nm (red) and 808 nm (near infrared) lasers, utilizing industrial colour camera. *Eur J Wood Prod* 81:1413–1426
- Tormanen V-MO, Mäkyänen AJ (2009) Detection of knots in veneer surface by using laser scattering based on the tracheid effect. In: 2009 IEEE instrumentation and measurement technology conference. IEEE, pp 1439–1443
- Trouy M-C (2015) Anatomie du Bois. Formation, fonctions et identification. (Wood anatomy. Formation, functions and identification). Éditions Quae
- Tsoulis G (1991) Science and technology of wood: structure, properties, utilization, vol 115. Van Nostrand Reinhold, New York
- Viguier J (2015) Classement mécanique des bois de structure. prise en compte des singularités dans la modélisation du comportement mécanique. (Mechanical grading of structural timber: considering

singularities in the modeling of mechanical behavior). PhD thesis, PhD thesis, Université de Lorraine

Publisher's Note Springer Nature remains neutral with regard to jurisdictional claims in published maps and institutional affiliations.